



RESEARCH PAPER

Maize ribosome-inactivating proteins (RIPs) with distinct expression patterns have similar requirements for proenzyme activation

Hank W. Bass^{1,*}, Julie E. Krawetz², Gregory R. O'Brien^{2,†}, Christopher Zinselmeier³, Jeffrey E. Habben³ and Rebecca S. Boston²

¹ Department of Biological Science, Florida State University, Tallahassee, FL 32306-4370, USA

² Department of Botany, Box 7612, North Carolina State University, Raleigh, NC 27695, USA

³ Trait and Technology Development, Pioneer Hi-Bred International, Inc., Johnston, IA 50131, USA

Received 25 February 2004; Accepted 5 July 2004

Abstract

Ribosome-inactivating proteins (RIPs, EC 3.2.2.22) are potent naturally occurring toxins found in numerous and diverse plant species. The maize RIP is unusual among the plant RIPs because it is synthesized as an inactive precursor (also known as maize proRIP1 or b-32). The proenzyme undergoes proteolytic activation that results in the removal of the NH₂-terminal, the COOH-terminal, and internal sequences to form a two-chain holoenzyme capable of irreversibly modifying the large rRNA. The characterization of a second maize RIP (RIP2), encoded by the gene designated *Rip3:2* is described here. Low levels of *Rip3:2* RNA were detected in roots, shoots, tassels, silks, and leaves, but the *Rip3:2* gene, unlike the *Rip3:1* gene, is not under the control of the transcriptional activator *Opaque-2*. Instead, its expression was up-regulated by drought. *Rip3:2* encodes a 31.1 kDa polypeptide that is very similar to proRIP1 in regions corresponding to those found in the active protein and the NH₂-terminal extension. A 19-amino-acid internal portion of proRIP2 has little similarity to the proRIP1 sequence except that both are very rich in acidic residues. RIP activity assays revealed that *Rip3:2* encodes a polypeptide that acquires RNA-specific *N*-glycosidase activity after proteolytic cleavage. Accumulation as inactive proenzymes may therefore be a general feature of maize RIPs. Differential regulation of the two RIP genes suggests that the corresponding proteins may be

involved in defence-related functions with one being regulated developmentally and the other being responsive to an environmental stimulus.

Key words: Maize, ribosome-inactivating protein, translation, toxin, water stress.

Introduction

Ribosome-inactivating proteins (RIPs, EC 3.2.2.22) are a class of translational inhibitors that share a site-specific RNA *N*-glycosidase activity (Barbieri and Stirpe, 1982; Stirpe *et al.*, 1992). Specifically, RIPs depurinate a universally conserved adenine residue of the large ribosomal RNA (A⁴³²⁴ of rat cytosolic 28S rRNA) (Endo *et al.*, 1987; Endo and Tsurugi, 1987) and make susceptible ribosomes impaired in translational elongation processes (reviewed in Wool *et al.*, 1992). Plant RIPs may function as antimicrobial or antiviral defence proteins, consistent with their usefulness in engineered plant disease resistance (Logeman *et al.*, 1992; Lodge *et al.*, 1993; Jach *et al.*, 1995; Hong *et al.*, 1996; Zoubenko *et al.*, 2000; Chen *et al.*, 2002; Yuan *et al.*, 2002; Kim *et al.*, 2003; Veronese *et al.*, 2003). Plant RIPs have also been used to develop therapeutic reagents with anti-HIV, anticancer, or immunomodulatory properties (Stirpe *et al.*, 1992; French *et al.*, 1995; Di Massimo *et al.*, 1997).

Plant RIPs are stable, basic (*pI* > 8) proteins found in a large number of species (Barbieri and Stirpe, 1982; Stirpe and

* To whom correspondence should be addressed. Fax: + 1 850 644 0481. E-mail: bass@bio.fsu.edu

† Present address: Department of Plant Pathology, North Carolina State University, Raleigh, NC 27695, USA.

Abbreviations: RIP, ribosome-inactivating protein; DAP, days after pollination; PAP, pokeweed antiviral protein; EST, expressed sequence tag; RFLP, restriction fragment length polymorphism.

Barbieri, 1986) as single-chain monomeric enzymes with apparent molecular masses of ~30 kDa (Type 1) or as two polypeptides in which one polypeptide with RIP activity (~30 kDa A-chain) is linked by a disulphide bridge to a carbohydrate-binding lectin (~30 kDa B-chain). The maize endosperm proRIP resembles a type 1 RIP because it is synthesized as a single polypeptide (33 kDa) without a lectin side chain, but it is unusual in being an acidic protein (pI 6.1) until it is activated by limited proteolysis. This proteolysis removes internal residues and leaves two polypeptide chains that are both required for *N*-glycosidase activity (Walsh *et al.*, 1991; Hey *et al.*, 1995). The name *Rip3:1* has been adopted for the gene referred to initially as 'b-32' (Soave *et al.*, 1981; Di Fonzo *et al.*, 1988) and later as 'maize RIP' (Walsh *et al.*, 1991), in accordance with the classification system reported by Mundy *et al.* (1994) for the Plant Gene Nomenclature Commission. The proenzyme form, proRIP1, is encoded by *Rip3:1* and is proteolytically activated to the mature form, RIP1. Proteins resembling the maize RIPs have also been identified in several close relatives of maize and in barley (Chaudhry *et al.*, 1994; Hey *et al.*, 1995).

Large-scale surveys for plant RIPs revealed that a wide variety of plants express RIPs (Gasperi-Campani *et al.*, 1985; Stirpe and Barbieri, 1986) and that some plants, including maize, express multiple RIPs (summarized by van Damme *et al.*, 2001). Because of their wide distribution and conserved enzymatic activity, RIPs have generally been presumed to make some important, albeit not fully understood, contribution to the plant (reviewed in Hartley and Lord, 1993; Hartley *et al.*, 1996; Nielsen and Boston, 2001; Veronese *et al.*, 2003).

Maize *Rip3:1* is one of the more thoroughly characterized RIP genes in terms of its regulation and expression within the plant. It was originally identified as an abundant, *Opaque-2*-regulated protein associated with endosperm development and was designated b-32 (Soave *et al.*, 1981). Subsequently, the product of the *Rip3:1* gene was shown to be a zymogen that was activated *in vivo* during seed germination and was designated proRIP (Walsh *et al.*, 1991; Bass *et al.*, 1992). In addition, biochemical, genetic, and molecular biological analyses have contributed to our understanding of the structure and expression of *Rip3:1*, as well as the activity of its gene product (Di Fonzo *et al.*, 1986, 1988; Hartings *et al.*, 1990; Lohmer *et al.*, 1991; Bass *et al.*, 1994; Muller *et al.*, 1997; Krawetz and Boston, 2000). The analysis of a second maize proRIP gene, designated *Rip3:2* (Bass *et al.*, 1995), is described here. It was found that the two maize RIP genes have very different expression patterns, but their gene products share structural and biochemical properties.

Materials and methods

Plant materials and treatments

Plants from the maize (*Zea mays* L.) inbred line W64A (W64A⁺) and its near isogenic mutant, *opaque-2* (W64A *o2*), were grown in the

greenhouse (Department of Botany, North Carolina State University, Raleigh, NC) or summer-season fields. Plant materials were harvested directly into liquid nitrogen except for root samples, which were briefly rinsed with H₂O to remove soil debris before freezing. Frozen samples were stored at -80 °C.

For the water-deficit microarray experiment, maize plants (Pioneer hybrid 3732) were propagated in a greenhouse in 15 l pots filled with an amended soil mixture composed of soil, sand, and Redi-earth™ (2:1:1 by vol.). The water deficit was created by a 'dry down' process, imposed when 100% of the tassels were beginning to exert through the whorl, which was 8 d prior to silk emergence. At this time, each pot was watered with 2.0 l of water, and this was the final watering plants would receive for 8 d, after which time a set of plants were rewatered. The experimental design was as follows: treatments were established in a randomized complete block design with four replicates of each of the three treatments. Unpollinated ears were collected at 8 d after initiation of the stress treatment (peak of water stress) and then 5 d after plants were rewatered (recovery phase). Control plants were not subjected to water stress. Morphometric determinations were made of ear growth, and then each ear was frozen immediately in liquid N₂.

For the immunoblot analysis of seed and leaf tissue, maize inbred line W64A was used as the genetic background. Endosperm tissue was dissected from kernels harvested 18 d after pollination. Seedlings were grown in 3" plastic pots and leaf tissue was harvested from well-watered plants or from drought-stressed plants in which watering had been withheld for 7 d. Seedling leaves were harvested and immediately frozen in liquid nitrogen.

Plasmid construction

The cloning and sequencing of a genomic clone for the maize *Rip3:2* gene was described by Bass *et al.* (1995). From an original bacteriophage isolate, λRip3:2, a 6.3 kb *Bam*HI restriction fragment was subcloned into pBluescript KS/+ (Stratagene, La Jolla, CA) to produce the plasmid designated pRip3:2, the source plasmid for all pRip3:2 subclones described here. A restriction map of the pRip3:2 insert was constructed by electrophoretic analysis of restriction fragments in agarose gels stained with ethidium bromide. Coding-region subclones were made from pRip3:2 by blunt-end ligation of the 874 bp *Pvu*II *Sca*I restriction fragment into the *Sma*I site of pBluescript KS/+ in either orientation. The resulting plasmids were designated pPST7 and pPST3 on the basis of the proximity of the 5' end of the gene to the vector promoters for T7 and T3 RNA polymerase, respectively.

Plasmids were also constructed that allow expression of recombinant protein with *N*-terminal histidine tags in *E. coli* BL21(DE3) cells (Novagen, Madison, WI). A *Bam*HI *Hind*III restriction fragment of pRIP3:2 that included the entire coding region was subcloned into the pRSET 5C expression vector (InVitrogen Corp., San Diego, CA) to give pECRip3:2. An expression clone (MOD1) encoding an active recombinant maize RIP1 (from the *Rip3:1* gene) and a modified zein clone, pMZ44-SV40, have been described previously (Wallace *et al.*, 1988; Krawetz and Boston, 2000).

Sequence homology analysis

Alignments of deduced amino acid sequences for several cloned RIPs were performed with the Genetics Computer Group software package (Wisconsin Package Version 10.3, Accelrys Inc., San Diego, CA). The primary structure alignment was generated with the GCG multiple sequence alignment program PILEUP with the parameters of matrix=blosom62, GapWeight=4 (gap creation penalty), and GapLengthWeight=1 (gap extension penalty). GenBank database accession numbers and regions of the deduced open reading frames are specified in the legend of Fig. 1 (see Results). The BLOCKS+ database (version 13.0) was searched for homology with the *Rip3:2*



Fig. 1. Comparison of amino acid sequences of RIP2 and other RIPs. The predicted open reading frame of *Rip3:2* (ZmR2) was aligned with seven other RIP sequences (ZmR1=entire ORF of maize RIP1, GenBank no. M83926 (Bass *et al.*, 1992); JP60=N-terminal 286 amino acids of barley JIP60, GenBank no. X66376 (Chaudhry *et al.*, 1994); Hv30=entire ORF of barley cRIP30, GenBank no. M62905 (Leah *et al.*, 1991); Trtn=entire ORF of tritin, GenBank no. D13795 (Habuka *et al.*, 1993); PAPL=entire ORF of pokeweed antiviral protein-leaf, GenBank no. X55383 (Lin *et al.*, 1991); RicA=ricin A-chain, GenBank no. X02388 (Lamb *et al.*, 1985); ShgA= α subunit of shiga toxin, Genbank no. M19437 (Strockbine *et al.*, 1988)). The stop codons are indicated with asterisks. Numbers above the alignments indicate the column number within the alignments, and numbers in parentheses refer to the conventional amino-acid labelling of the ricin A-chain (Lamb *et al.*, 1985; Montfort *et al.*, 1987). The 1–2-residue-wide vertical black areas mark residues showing complete identity in this alignment. The dots above ZmR2 mark conserved residues that are common to six or more of the eight sequences in this alignment. The five conserved active-site-cleft residues (Y80, Y123, E177, R180, W211) that are found in bacterial as well as plant RIPs are indicated in parentheses (Katzin *et al.*, 1991). The conserved sequence blocks from the Blocks Database (Henikoff and Henikoff, 1994) are drawn as boxes around ZmR2 and labelled (Block A through E, as specified by RIP Block set IPB001574). The lower-case letters of the proRIP1 (ZmR1) sequence indicate amino acids determined by Walsh *et al.* (1991) to be missing after proteolytic activation. The NH₂-terminal and COOH-terminal residues shown for ricin A-chain represent the terminal amino acids found in the native protein.

ORF with the BLOCKS WWW Server (www.blocks.fhrc.org) (Henikoff and Henikoff, 1994). The sequences corresponding to the RIP Blocks (IPB001574 Blocks A through E) and labelled (see Fig. 1 in the Results).

DNA isolation and Southern blot analysis

Bacteriophage DNA used for comparison of cloned DNAs with genomic restriction fragments was isolated from λ Rip3:2 according to the method of Maniatis *et al.* (1982). Maize DNA was purified from 3–5 cm ear-shoots. The method of Zimmer and Newton (1982) was scaled up to accommodate larger samples and was carried out through the step for proteinase K treatment. DNA was subsequently purified by isopycnic centrifugation in caesium chloride as described by Maniatis *et al.* (1982).

For copy-number reconstructions, 2×10^6 haploid genome equivalents of DNA were loaded per single-copy lane (10.6 μ g maize DNA, 2.02×10^{-11} g plasmid DNA) on the basis of a 1C value of 5.3 pg for maize DNA. Undigested lambda DNA was added to plasmid and bacteriophage DNAs to allow loading of 1 μ g total DNA per lane.

DNA gel blots were performed according to the technique of Southern (Southern, 1975), and the filters were hybridized in aqueous buffers containing $1 \times$ SSC at 68 °C as described by Bass *et al.* (1994).

RNA isolation and gel blot analysis

Maize RNA was isolated from developing kernels as described by Langridge *et al.* (1982). Other RNAs were isolated by the phenol/SDS method for plant RNA preparation (Ausubel *et al.*, 1992), modified by the addition of polyvinyl pyrrolidone and polyvinyl-polypyrrolidone (Sigma, St Louis, MO) to 1% (w/v) each in the initial grinding buffer and addition of a LiCl precipitation step (4 M LiCl, 4 °C, 12 h) following resolubilization of the pellet collected after precipitation using isopropyl alcohol. RNA was isolated from tissues that were quick-frozen in liquid nitrogen. All RNAs on the gel blot (except for kernel o2 and shoot) were from field-grown inbred line W64A. RNA was isolated from the following tissues, in order of their appearance: 'kernel +', 20 d after pollination (DAP) whole kernel of the normal (+) line; 'kernel o2', same as kernel + except homozygous recessive for *opaque-2* (line W64A o2); 'shoot, seedling', shoots harvested from

W64A⁺ seedlings grown in vermiculite and harvested 9 d after planting; 'leaf, young', leaves from inside the whorl, light green, harvested at 17.00 h; 'leaf, mature', healthy adult leaves, harvested at 11.00 h; 'husk', husks from an ear with newly emerging silks, harvested at 11.00 h; 'silk', whole silks from ear with newly emerged silks, harvested at 11.00 h; 'tassel, pre-emerged', pre-emergence tassel shoot from a 5' tall plant, harvested at 13.00 h; 'tassel, shedding', whole tassel from a plant that had shed over approximately half of its pollen, harvested at 11.00 h.

Synthetic RNAs for use as positive and negative specificity controls were transcribed *in vitro* with T3 RNA polymerase according to the manufacturer's instructions (Ambion, Inc., Austin, TX). Input template DNA was from *Bam*HI-digested pPST3 to produce a *Rip3:2* transcript or from *Xba*I-digested pZmcRIP-3 to produce a *Rip3:1* transcript (Bass *et al.*, 1992). These control RNAs were then purified by phenol/chloroform phase extractions, treated with DNase for removal of the template, and quantified by UV absorbance spectroscopy.

RNA gel blots were prepared and used in hybridization experiments as previously described (Bass *et al.*, 1994) and probes were radiolabelled as described by Bass *et al.* (1992). The amount of RNA loaded for the gel blot was 5 µg per lane for kernel, 1 ng per lane for synthetic, and 12 µg per lane for all other RNAs. From the same sample tubes, a duplicate gel was loaded at 1/6th the amount, subjected to electrophoresis, stained with acridine orange (at 10 µg ml⁻¹) and photographed for verification of the integrity and relative amounts of total RNA. The *Rip3:2*-specific probe was made from a 90 bp *Rma*I fragment cleaved from a 250 bp *Hinc*II subclone of pRip3:2. The stringency of hybridization was estimated to be $T_m - 8^\circ\text{C}$ as calculated according to the formula $T_m = 81.5^\circ\text{C} + 16.6 \times \log\{\text{salt}\} + 0.41(\%G + C) - 650/L$, where L is the average nucleotide length of the probe and $\{\text{salt}\}$ is the molar concentration of monovalent cation (Wetmur and Davidson, 1968; Casey and Davidson, 1977).

RNA mapping

Primer-extension experiments were performed essentially as described previously except that reverse transcription reactions were carried out at 37 °C for 60 min (Ausubel *et al.*, 1992). The synthetic DNA oligonucleotide, 5'-GGTGCAGTGTGATCAC-3' (PE in Fig. 2C), was 5' end-labelled with γ -³²P-ATP by T4 polynucleotide kinase and used as a primer for the reaction. *Hae*III restriction fragments from pBluescript KS/+ were end-labelled and used as molecular-weight markers.

For S1 nuclease protection experiments, the *Sma*I *Bcl*II restriction fragment of pRip3:2 was treated with shrimp alkaline phosphatase (US Biochemical Corp., Cleveland, OH), which removed terminal phosphates. The fragment was then 5' end-labelled with γ -³²P-ATP and T4 polynucleotide kinase to a specific activity of 2×10^5 cpm pmol⁻¹ 5' ends. The radiolabelled fragment was cleaved with *Ssp*I, gel-purified, and used in S1 nuclease protection assays (8×10^4 cpm per reaction) as described by Boston and Larkins (1986). Approximate sizes of the protected DNAs were determined by comparison with marker DNA sequencing products fractionated on the same gel.

Expression profiling

Microarray slides contained 384 maize ESTs (plus controls) that represent genes from pathways involved in carbohydrate metabolism, cell cycle regulation, phytohormone metabolism, signalling, and stress responses. Plasmid DNA for each target EST was amplified with M13R and M13F primers. The amplified products were purified with the Qiagen 96-well PCR product purification kit, and the DNAs were spotted onto MD Type VII slides by means of DMSO binding chemistry according to the manufacturer's protocols (MD/Amersham, www.apbiotech.com). Each EST was repeated eight times on a slide.

Poly(A⁺) RNA was isolated from immature ear tissue with a combination of Trizol (Gibco-BRL), Qiagen, MACS (Miltenyi

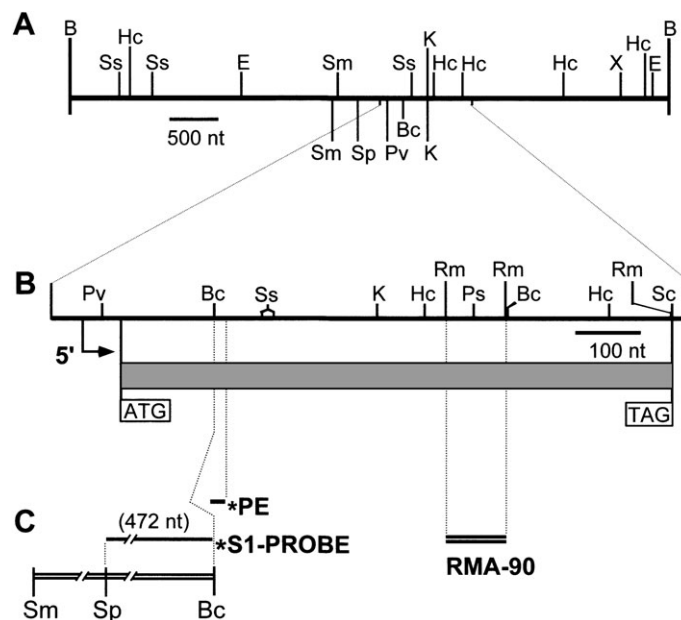


Fig. 2. Schematic representation of the *Rip3:2* gene and hybridization probes. (A) Restriction map of pRip3:2. Restriction enzyme cleavage sites were determined by electrophoretic analysis (sites labelled above the line) or by DNA sequencing (sites labelled below the line in (A); all sites in B and C). The positions (in kb) of the gel-based sites relative to the *Bam*HI site shown at left are *Bam*HI (B 0, 6.26), *Sst*I (Ss 0.52, 0.87, 3.58), *Hinc*II (Hc 0.63, 3.8, 4.1, 5.15, 6.0), *Eco*RI (E 1.8, 6.09), *Sma*I (Sm 2.79), *Kpn*I (K 3.73), and *Xba*I (X 5.75). Other restriction-enzyme cleavage sites are indicated as follows: *Ssp*I (Sp), *Pvu*II (Pv), *Bcl*II (Bc), *Rma*I (Rm), *Pst*I (Ps), and *Sca*I (Sc). (B) Restriction map of the 963 bp region of pRip3:2 derived from the region of the clone for which DNA sequence is available (GenBank no. L26305). Positions of the start (ATG) and stop (TAG) codons of the predicted ORF are noted. (C) Map of restriction fragments and oligonucleotides (PE) used as radioactive probes in this study. For end-labelled DNAs, position of label on the strand complementary to mRNA is marked with an asterisk.

Biotec), and FastTrack (Invitrogen) RNA isolation kits. Probes were labelled with Cy3-dCTP or Cy5-dCTP and 1 µg of poly(A+) RNA per reaction. Labelling, hybridization, and washing steps were carried out as recommended by MD/Amersham (www.apbiotech.com). Slides were placed in an image-analysis scanner, and the amount of fluorescence given off by each spot was determined (ArrayVision, Imaging Research, Inc.). This value was then used to calculate the differences in message levels of particular genes between water-deficient and well-watered (control) tissues. Cy3 and Cy5 dye signal was first normalized by regression analysis, and analysis of variance (ANOVA) was conducted on these adjusted values. Dye, replicate, spot, and plant variability was adjusted by analysis of variance, and Fisher's *t*-test was used to test differences between means.

Protein purification and immunodetection

Recombinant proteins were produced and purified as described by Krawetz and Boston (2000). Immunoblot analysis of recombinant proteins was carried out on proteins fractionated by SDS-PAGE, electroblotted, and probed with anti-proRIP1 antibodies as described by Bass *et al.* (1992). Immunodetection was performed with antirabbit secondary antibody conjugated to alkaline phosphatase. Cross-reacting material was visualized by colorimetric detection with Western Blue reagent according to the manufacturer's instructions (Promega Corp., Madison, WI).

Plant protein extracts were obtained by homogenization of liquid-nitrogen frozen leaf tissue with 50 mM TRIS-HCl, pH 6.8, centrifugation for 10 min at 16 100 *g* at 4 °C, and collection of the resulting supernatant. The protein concentrations were determined using Coomassie Plus (Pierce), fractionated through 12% SDS-polyacrylamide gels, and transferred to nitrocellulose filters (according to the manufacturer's procedures). Polyclonal anti-RIP1 antibody was purified over a column of recombinant His-tagged proRIP1 coupled to cyanogen-bromide activated Sepharose. Western blots were carried out with affinity-purified anti-RIP antibody diluted 1:333 followed by application of anti-rabbit secondary antibody conjugated to horseradish peroxidase and then visualized with Supersignal West Femto reagent (Pierce).

RIP activity assays

Purified rRIP2 or kernel proRIP1 was treated with 3 µg ml⁻¹ papain (Boehringer Mannheim, Indianapolis, IN) for 15 min at room temperature. Papain was subsequently inactivated by addition of the inhibitor E-64 to 5 µM (Sigma, St Louis, MO). RIP activities were measured in translational inhibition assays or aniline cleavage assays for RIP-specific RNA modification as described previously (Bass *et al.*, 1992).

RIP activity of protein synthesized *in vitro* was assayed by adding a second transcript and measuring the relative amount of protein produced from it essentially as described by May *et al.* (1989), except that both ³H-leu and ³⁵S-met were included in the translation reactions. The synthetic transcripts were synthesized from MOD1 and pPST7 with T7 RNA polymerase and pMZ44-SV40 with SP6 RNA polymerase according to the manufacturer's instructions (Promega Corp., Madison, WI). A further modification of the procedure was that translation was carried out for 30 min prior to addition of the second transcript in 4-fold excess of the first. Protein synthesis directed by the second transcript was measured over time.

Results

A second ribosome-inactivating protein gene from maize, Rip3:2

By screening maize genomic libraries at moderate stringency with a full-length endosperm *Rip3:1* cDNA clone,

a cross-hybridizing DNA fragment that was different from *Rip3:1* was isolated repeatedly. Subsequent determination of the DNA sequence from one of these genomic clones allowed an open reading frame of 278 amino acids to be predicted (GenBank protein accession AAC41650). The DNA cloning and sequencing of this gene are described by Bass *et al.* (1995), and the gene has been designated *Rip3:2*.

The amino-acid sequence deduced from the ORF of the *Rip3:2* clone was compared with sequences of several diverse and representative proteins. Figure 1 shows an alignment of amino-acid sequences of the endosperm RIPs of maize, barley, and wheat (ZmR1, Hv30, and Trtn, respectively); the catalytic portion of a type 2 RIP from castor bean (RicA); the leaf RIPs from barley and pokeweed (JP60 and PAPL); and the evolutionarily distant microbial RIP shiga toxin (ShgA), from *Shigella dysenteriae* (Lamb *et al.*, 1985; Strockbine *et al.*, 1988; Leah *et al.*, 1991; Lin *et al.*, 1991; Bass *et al.*, 1992; Becker and Apel, 1992; Habuka *et al.*, 1993).

Although the degree of amino-acid sequence conservation among RIPs varies widely between and within species, the conservation of active site cleft residues is strictly conserved (Evensen *et al.*, 1991; Fordham-Skelton *et al.*, 1991; Funatsu *et al.*, 1991; Legname *et al.*, 1991; Lin *et al.*, 1991; Poyet *et al.*, 1994). The predicted ORF of *Rip3:2* exhibits the sequence features typical of a functional RIP. It contains the five residues (Fig. 1; Y80, Y123, E177, R180, W211) that reside in the active site cleft of the ricin A-chain as determined by X-ray crystallography and mutagenesis studies (Montfort *et al.*, 1987; Frankel *et al.*, 1989; Katzin *et al.*, 1991; Ready *et al.*, 1991; Weston *et al.*, 1994). In addition, the *Rip3:2* ORF showed highly significant, independent matches to blocks obtained from searches against the BLOCKS+ database with the *Rip3:2* ORF. This database is useful for identifying meaningful homologies among proteins with poor overall sequence similarity (Henikoff, 1991; Henikoff and Henikoff, 1994). The *Rip3:2* ORF showed highly significant alignments with the 'Ribosome-inactivating protein' blocks set IPB001574 (Henikoff and Henikoff, 1994). Most of the invariant and highly conserved residues fall within one or another of the RIP blocks.

The maize endosperm protein proRIP1 (Fig. 1, ZmR1) undergoes a proteolytic activation that involves removal of amino acids from both termini as well as an internal acidic region (Walsh *et al.*, 1991). Intriguingly, the *Rip3:2* ORF also has an internal stretch of amino acids that is similar in its position (between Blocks C and D) and highly acidic chemistry to the internally processed region of proRIP1. In this same region, a barley RIP proenzyme, JIP60, also shows extra acidic residues (Chaudhry *et al.*, 1994). Both maize proRIP1 and the barley leaf RIP, JIP60, undergo proteolytic activation involving breaks in the polypeptide chain (Walsh *et al.*, 1991; Chaudhry *et al.*, 1994). The

similarities in sequence organization of the three RIPs suggested that the RIP2 protein was a proRIP zymogen that could be activated by protease treatment.

Genomic Southern blot analysis of maize RIPs

To characterize the *Rip3:2* gene, the restriction map of a plasmid containing the full-length genomic clone, pRip3:2, was determined. Figure 2A shows the map for a 6 kb *Bam*HI fragment of the genomic clone. Figure 2B shows the region for which the DNA sequence was determined (Bass *et al.*, 1995). This region encodes a single, continuous ORF, indicative of an intron-free gene.

To confirm that the cloned fragment present in pRip3:2 represented the organization of that DNA in the maize genome, a genomic Southern blot analysis was carried out. Figure 3 shows results that allowed the correspondence of cloned and genomic restriction fragments for *Rip3:2* to be verified. The DNAs from plasmid pRip3:2, maize leaf, and the bacteriophage isolate, λ Rip3:2, were cleaved with *Eco*RI, *Bam*HI, or *Hind*III (lanes E, B, and H, respectively). Hybridizations were carried out at moderate stringencies with a radiolabelled maize *Rip3:1* cDNA clone to allow detection of multiple maize RIP genes (Bass *et al.*, 1992). Only one major band per lane (4.3 kb *Eco*RI, 6.3 kb *Bam*HI, and 4.0 kb *Hind*III) was detected from the λ Rip3:2 genomic clone. A corresponding set of bands was identified in the lanes containing maize DNA (marked with circles). The 6.3 kb *Bam*HI band represents the fragment shown in Fig. 2A. These results indicated that the genomic clone containing *Rip3:2* had not undergone any major rearrangements during cloning. Additional bands were observed to be approximately 18 kb and 30 kb in the *Eco*RI-digested DNA, 5.5 kb in the *Bam*HI-digested DNA, and 2.15 kb in the *Hind*III-digested DNA. These fragments were presumed to harbour the *Rip3:1* gene (Di Fonzo *et al.*, 1988;

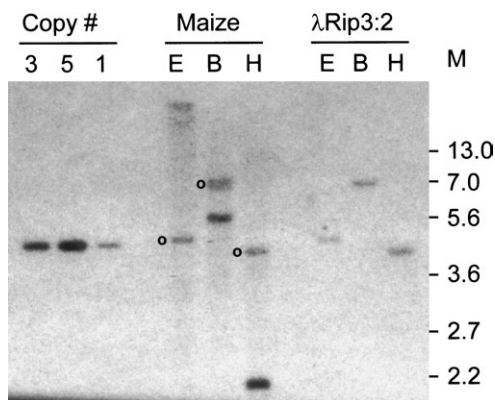


Fig. 3. Southern blot analysis of *Rip3:2*. DNA from pRip3:2 was cleaved with *Eco*RI and loaded in copy number equivalents (Copy numbers=3, 5, 1 as noted above lanes). DNAs from genomic clone λ Rip3:2 or maize were digested with *Eco*RI (E), *Bam*HI (B), or *Hind*III (H). Molecular weight markers (M) are indicated at right in kb. Bands from maize DNA corresponding to those from λ Rip3:2 are marked with circles.

Hartings *et al.*, 1990). By comparing signal strengths from copy number reconstructions of plasmid DNA with those in the maize genomic DNA lanes, it was determined that the maize *Rip3:2* sequence (bands marked with circles) was present at approximately one copy per haploid genome.

Expression of the *Rip3:2* RNA

The conservation of amino acid sequence between RIP1 and the deduced ORF of *Rip3:2* raised the question of whether previous characterization of proRIP/b-32 gene expression was confounded by the presence of gene products from *Rip3:2* (Di Fonzo *et al.*, 1988; Hartings *et al.*, 1990; Bass *et al.*, 1992; Muller *et al.*, 1997). To investigate the expression of the *Rip3:2* gene, a 90 bp *Rma*I restriction fragment was identified (Fig. 2C) that could be used at high stringency to detect RNA from *Rip3:2* but not *Rip3:1*. This fragment shares only 65% nucleotide sequence identity with *Rip3:1*. RNAs were isolated from a variety of plant parts and subjected to gel blot analysis. Hybridizations were carried out at a high stringency to prevent annealing of sequences with greater than 10% mismatch (Bonner *et al.*, 1973). Unexpectedly, it was found that RNA homologous to *Rip3:2* was present at low levels in many different tissues, as shown in Fig. 4. Specifically, distinct signals (arrow, Fig. 4) were observed for RNA prepared from tassel, silk, husk, leaf, shoot, and root. Of all the RNAs assayed with the gene-specific *Rip3:2* probe, the

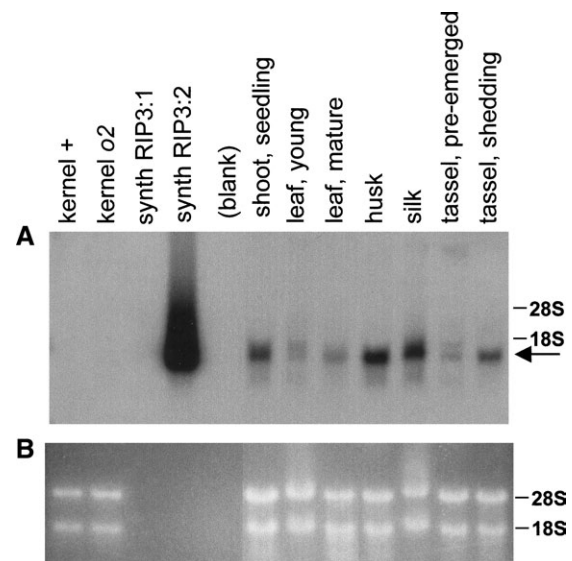


Fig. 4. Accumulation of *Rip3:2* RNA throughout the plant. (A) An RNA gel blot was incubated with the radiolabelled *Rip3:2* gene-specific probe, RMA 90. RNA was purified from the plant parts indicated above the lanes and loaded in equal amounts ($5 \mu\text{g lane}^{-1}$ for kernel, 1 ng lane^{-1} for synthetic, and $12 \mu\text{g lane}^{-1}$ for all others). The autoradiograph shown here was exposed for 16 d at -80°C with an intensifying screen. The positions of *Rip3:2* RNA (arrow), and the large (28S) and small (18S) rRNAs are indicated on the right. (B) A duplicate RNA gel was loaded and acridine-orange-stained as a loading control. The positions of the large (28S) and small (18S) rRNAs are indicated on the right.

kernel RNAs showed the least signal and did not result in a band on the long exposure (380 h) shown (Fig. 4A). For comparison, the *Rip3:1* gene is known to be endosperm-specific and would be expected to show a very strong hybridization signal in RNA from normal kernels (Fig. 4, kernel +) and a reduced but detectable signal in RNA from *opaque-2* kernels (Bass *et al.*, 1994). The *Rip3:2* RNA accumulation pattern is therefore fundamentally different from that of *Rip3:1*. The gene-specific hybridization conditions were verified with internal controls of synthetic RNAs corresponding to either *Rip3:1* or *Rip3:2* (Fig. 4, synth lanes). A very strong signal was obtained with *Rip3:2* RNA, but no detectable hybridization was observed with *Rip3:1* RNA. These results were taken to indicate that *Rip3:2* is an active gene and that the corresponding RNA products are present in such low amounts in kernels that they are unlikely to have affected results of previous studies (Bass *et al.*, 1992, 1994) of the abundant *Opaque-2*-regulated seed proRIP1.

Primer extension and S1 nuclease mapping of *Rip3:1* and *Rip3:2* genes

To discriminate better between the *Rip3:1* and *Rip3:2* transcripts, two different assays were performed. For primer-extension assays, an 18-base oligonucleotide complementary to RNA from both maize RIP genes was end-labelled with γ - ^{32}P -ATP and used as a primer for reverse transcription (PE probe in Fig. 2C). The results are presented in Fig. 5, and the sources of the RNA are listed above the lanes. Total RNA from maize kernels harvested at 20 DAP directed synthesis of a distinct extension product of ~212 nt (Fig. 5A, kernel). The presence of *Rip3:2* RNA in roots was demonstrated by detection of a slightly larger ~216 nt band (Fig. 5A, root). Leaf, silk, and tassel also showed this ~216 nt extension product (HW Bass and RS Boston, unpublished results). The ~212 nt extension product from kernel RNA was most probably derived from the abundant *Rip3:1* RNA template, whereas the larger ~216 nt transcription product in reactions containing root RNAs probably complemented *Rip3:2* RNA. Primer extension reactions containing 0.1 and 0.5 ng of synthetic RNA from a *Rip3:2* clone included as controls produced the expected ~216 nt extension product (HW Bass and RS Boston, unpublished results). The ~216 nt fragment predicts a transcriptional start site at or near a G residue (position 43 of the GenBank sequence accession no. L26305) that is 58 nt upstream of the predicted translational start codon.

To confirm that the two different primer extension products were derived from different RIP RNAs, an S1 nuclease protection assay was performed. RNAs isolated from seedlings, or RNAs synthesized *in vitro*, were allowed to anneal with a DNA probe radiolabelled at the 5' end (Fig. 2C, S1-probe). Regions of the probe protected from nuclease degradation were analysed on denaturing poly-

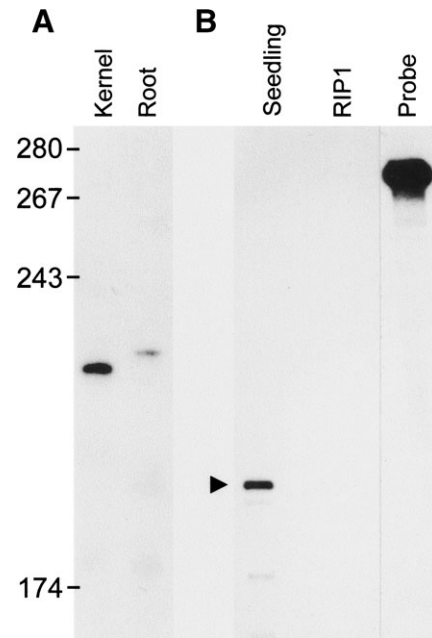


Fig. 5. 5' mapping of *Rip3:2* transcripts. (A) Primer extension analysis of *Rip3:2* RNAs (30 μg) were annealed to the ^{32}P -end-labelled PE probe oligonucleotide (5×10^3 cpm) and extended with reverse transcriptase. An autoradiograph of extension products from kernel and root RNA is shown with positions of molecular weight markers noted at left. (B) S1 nuclease protection assay. Reactions were carried out in the presence of seedling RNA or synthetic *Rip3:1* RNA. The intact probe and primary protected product (arrow) are noted.

acrylamide gels alongside radiolabelled molecular-weight markers. Within the region expected to be protected by a homologous probe, *Rip3:1* and *Rip3:2* sequences showed several differences, including a 3 nt insertion in *Rip3:2*, three adjacent mismatched residues, and several single-nt mismatches. Thus, a *Rip3:2* probe would not be expected to protect the full *Rip3:1* sequence from S1 nuclease cleavage.

One major transcript in seedling RNA was protected by the *Rip3:2* probe (Fig. 5B, arrowhead). Comparison with markers fractionated on the same gel allowed the size of the protected fragment to be determined, ~205 nt, a size that is consistent with the predicted transcriptional start site as a G residue 58 nt upstream of the predicted translational start site. No long protection products were visible in lanes containing synthetic *Rip3:1* RNA (lane Rip3:1) or buffer alone (data not shown). Inclusion of synthetic *Rip3:2* RNA resulted in protection along the full length of the synthetic RNA (GR O'Brien and RS Boston, unpublished results).

Induction of *Rip3:2* RNA expression by water stress

The widespread but relatively low expression of *Rip3:2* throughout the plant resembles that of constitutive or housekeeping genes, but RIPs from a number of plants have been shown to be inducible by both biotic and abiotic stresses, including methyl jasmonate, water stress, ABA, ethylene, mechanical wounding, heat, cold, salt, and

pathogens (reviewed in Nielsen and Boston, 2001; see also Park *et al.*, 2002). The effect of a water deficit on the *Rip3:2* gene was examined by DNA microarray analysis of RNA from unpollinated maize ears. Table 1 shows the effect of an 8 d water deficit on ear growth. The water-deficit decreased ear-shoot fresh weight by 56%, ear fresh weight by 56%, ear length by 26%, ear volume by 53%, and ear diameter by 25%. Gene expression in ears was determined at the peak of stress as well as 5 d after plants were rewatered to allow recovery from the stress. *Rip3:2* showed transcript levels in stressed ears 48-fold higher than those in well-watered ears (Table 2). After rewatering, water-deficit treatment and control ears did not differ in RIP2 expression. As a means of comparison, the expression pattern of two other genes encoding *rab17* (dehydrin 3) and an *aquaporin* (Chevalier *et al.*, 1995) is also shown. Expression of *rab17* has been shown by others (Vilardell *et al.*, 1990) to be very responsive to water-stress conditions, and in this experiment a greater than 200-fold increase was measured in *rab17* gene expression upon stress. By contrast, *aquaporin* RNA levels decreased in response to the 8 d water-stress treatment. Like *Rip3:2*, both genes returned to basal levels of expression upon recovery after rewatering. Similar results for *Rip3:2* gene expression were obtained with

Table 1. Effect of an 8 d water deficit on ear growth traits

For the water-deficit treatment, water was withheld for 8 d prior to silk emergence. Data presented are those collected on the day of silk emergence, \pm standard deviation. The ear shoot is composed of the shank, husk, and ear (cob and ovaries).

Trait	Control	Water stress
Ear shoot fresh weight (g per ear shoot)	61 \pm 24	27 \pm 11
Ear fresh weight (g per ear)	18 \pm 7	8 \pm 4
Ear length (mm per ear)	137 \pm 16	101 \pm 14
Ear volume (ml per ear)	17 \pm 9	8 \pm 4
Ear diameter (mm per ear)	16 \pm 2	12 \pm 2

Table 2. Expression profile data for *Rip3:2*

For the water-deficit treatment, water was withheld 8 d prior to silk emergence (8 d of stress), then unpollinated ears from some of the stressed plants were sampled along with ears from well-watered (control) plants. The remaining stressed plants were rewatered and 5 d later unpollinated ears from these plants were sampled (5 d after rewatering). Poly (A⁺) RNA was isolated from ear samples and labelled with Cy3-dCTP or Cy5-dCTP. The labelled cDNA probes were allowed to hybridize with 384 maize ESTs spotted onto glass slides, and the resulting hybridization signals were quantified with a microarray scanner. The fold change in signal was calculated for three genes (*Rip3:2*, *rab17*, and *aquaporin*) after 8 d of water deficit, and 5 d after the rewatering recovery.

Gene	8 d of stress		5 d after rewatering	
	Fold change (stress/control)	Probability	Fold change (rewater/control)	Probability
<i>Rip3:2</i>	48.0	0.01	0.0	0.16
<i>rab17</i>	204.4	0.01	0.0	0.12
<i>Aquaporin</i>	-1.9	0.05	0.0	0.15

other expression-profiling platforms (JE Habben and C Zinselmeier, unpublished results).

Cross-reactivity of maize RIPs

The amino acid similarity between the ORFs of *Rip3:1* and *Rip3:2* suggested that the two proteins would have similar antigenic epitopes, but the multiple RIPs produced by many plant species have distinct antigenic cross-reactivity (Irvin *et al.*, 1980; Barbieri *et al.*, 1982; Falasca *et al.*, 1982; Massiah and Hartley, 1995; Hao *et al.*, 2001). An immunoblot assay was used to investigate cross-reactivity between the recombinant proRIP2 protein and anti-proRIP1 antiserum. Figure 6 shows the signals obtained from equal amounts of proRIP1 purified from kernels and recombinant proRIP2 (rproRIP2) produced in *E. coli*. The two polypeptides are expected to differ slightly in size because the longer internal and NH₂-terminal regions of the proRIP1 zymogen are partially offset by a 45 amino acid NH₂-terminal fusion peptide in the recombinant proRIP2. Both proRIP1 and proRIP2 migrated through the SDS gels to positions consistent with the predicted size differences between the two proteins. In addition, because both showed strong cross-reactivity with the anti-RIP1 antibody, it was possible to use the antibody to assay for proRIP2 protein in plant extracts.

Induction of proRIP2 protein levels by water stress

It has previously been found that the RIP1 mRNA and protein levels show similar accumulation kinetics (Bass *et al.*, 1992). Because the *Rip3:2* mRNA was induced dramatically in water-stressed plants, immunoblots and affinity-purified antibodies that detect both proRIP1 and proRIP2 were used to probe for proRIP2 in protein from water-stressed plants. It was observed that the application of a dehydration stress resulted in the appearance of a band (Fig. 7A, lane 4) which was attributed to the presence of proRIP2. This band is visible in both control and water-stressed leaves, but the signal is significantly stronger after water stress (Fig. 7, compare lanes 3 and 4). For comparison,

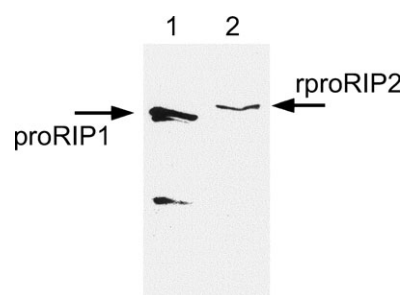


Fig. 6. Cross-reactivity of maize RIPs. Equal amounts of proRIP1 purified from kernels (lane 1) and rproRIP2 made in *E. coli* (lane 2) were fractionated by SDS-PAGE, electroblotted, and incubated with anti-proRIP1 antibodies as described by Bass *et al.* (1992). Immunodetection was with an alkaline phosphatase colorimetric assay.

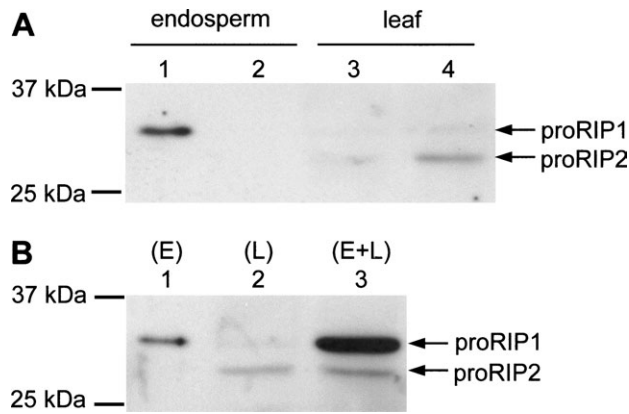


Fig. 7. Immunoblot analysis of RIP1 and RIP2 from plant tissues. Soluble proteins from endosperm and leaf tissues were immunoblotted as described in legend to Fig. 6. The positions of the molecular weight markers are indicated on the left, and the assignments of the major bands detected are indicated on the right. (A) Lanes contained 0.17 μg protein lane⁻¹ for the endosperm samples (lane 1, normal; lane 2, *opaque-2*) or 50 μg protein lane⁻¹ for the leaf samples (lane 3, unstressed; lane 4, water-stressed). (B) Sample mixing experiment in which protein from normal endosperm (lane 1) and leaf tissue (lane 2) were mixed (lane 3) to show the electrophoretic resolution of the proRIP1 and proRIP2 bands.

endosperm tissue was included from which *Opaque-2* induced proRIP1 is known to accumulate (Fig. 7, lane 1). A mixing experiment (Fig. 7B, lane 3) demonstrates that the detected bands from endosperm and leaf do not comigrate. The proRIP1 and proRIP2, therefore, can be resolved under these gel conditions. The interpretation that proRIP2 is the predominant immunodetectable species from water-stressed leaves is consistent with the findings from the gene-specific RNA gel blot data (Fig. 4) and the expression profiling data (Table 2).

Enzymatic activity of RIP2

To determine whether or not the *Rip3:2* clone encoded a protein with RIP activity, it was used to direct synthesis of recombinant protein in *E. coli*. The *E. coli* expression strategy was chosen so that it was possible to ensure that RIP1 was absent from the reaction. The recombinant proRIP2 protein has a 34-amino-acid NH₂-terminal extension containing a polyhistidine tag from the cloning vector and 11 amino acids from the 5' untranslated region immediately upstream of the *Rip3:2* start codon. Purified rproRIP2 was assayed in a cell-free translational inhibition assay (Bass *et al.*, 1992). Figure 8 shows the dose-response curves for protein synthesis in rabbit reticulocyte cell-free translation reactions preincubated with RIPs. Addition of the untreated form of rproRIP2 did not inhibit translation in the cell-free system (Fig. 8, squares). Treatment of the rproRIP2 protein with papain, however, resulted in a dramatic activation of the enzyme (Fig. 8, circles; ID₅₀ = 1.2×10^{-5} $\mu\text{g ml}^{-1}$). The papain-treated rproRIP2 had lower translational inactivation activity than did papain-treated proRIP1 from kernels (Fig. 8, diamonds).

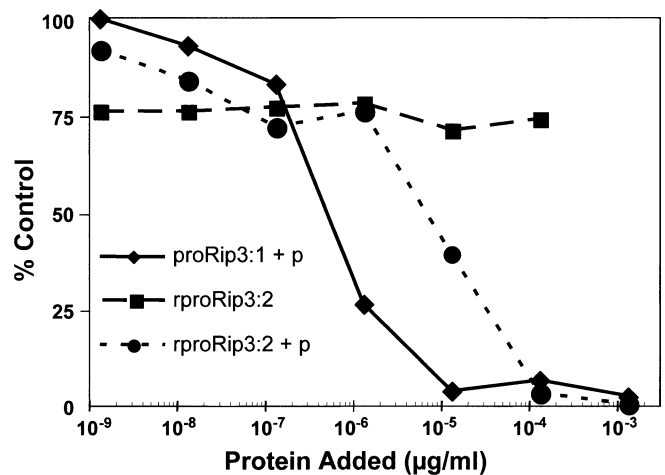


Fig. 8. Translational inhibition by protease-treated recombinant proRIP2. Recombinant RIP2 (rproRIP3:2) purified from *E. coli* and native proRIP1 (proRIP3:1) purified from maize kernels were treated with papain (+ p) and preincubated with rabbit reticulocyte lysates prior to initiation of translation. A duplicate reaction containing rRIP2 was treated similarly except that papain treatment was omitted (rproRIP3:2). TCA-precipitable radioactivity in each sample was normalized to a control (1.6×10^7 cpm ml⁻¹) with no RIP added.

To confirm that the translational inhibition was due to RIP-specific modification of the rabbit ribosomes, a diagnostic aniline cleavage reaction was performed. Depurination of the large rRNA by RIPs renders the rRNA susceptible to strand scission by aniline at the point of depurination. Such cleavage generates a 3' terminal rRNA fragment of approximately 400 nt that can be visualized after electrophoretic fractionation and ethidium-bromide staining (Peattie, 1979). RNA modification assays were performed with either papain-activated rproRIP2 or an active form of RIP1 and target ribosomes from a rabbit reticulocyte cell-free translation lysate. Subsequent purification of RNA, treatment with aniline, and fractionation through a denaturing polyacrylamide gel yielded the ~ 425 nt products visible in Fig. 9. In controls lacking aniline (Fig. 9, lanes 1 and 3) the diagnostic band was not detectable. The *Rip3:2* gene therefore encodes the proenzyme form of a ribosome-inactivating protein, and the treatment of rproRIP2 with papain results in the RNA *N*-glycosidase activity that is characteristic of all RIPs.

The dependence of rproRIP2 on proteolysis for enzymatic activity suggested that the primary polypeptide produced from a non-recombinant *Rip3:2* mRNA might be an inactive zymogen. To test this idea a subclone (from pPST7) of the intron-free *Rip3:2* genomic clone was used as a template to make a full-length transcript *in vitro* containing the presumed native *Rip3:2* ORF. This synthetic transcript was translated *in vitro* for 30 min, and then a second unrelated transcript was added as a translational reporter. The reporter transcript encoded a 36 kDa fusion protein consisting of a 19 kDa zein storage protein with a 17 kDa insertion from the SV40 VP2 protein (Wallace

et al., 1988). It was predicted that if RIP2 was synthesized as an inactive zymogen, then its presence would not inhibit the translation of the subsequently-added zein reporter transcripts. The results of this experiment are shown in Fig. 10. First, reporter protein synthesis (zein, from the second transcript) was visualized from a control experiment in

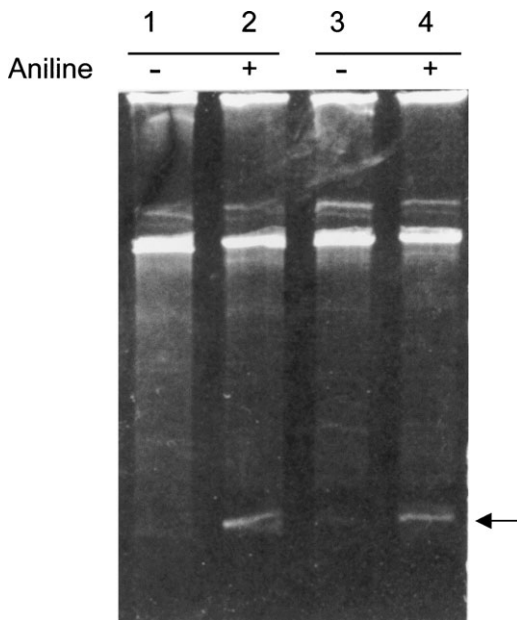


Fig. 9. Aniline cleavage of rRIP2-modified RNA. RNA isolated from RIP-treated rabbit reticulocyte lysates was separated through a 4.5% denaturing polyacrylamide gel and visualized by ethidium bromide staining. Reactions contained rRIP2 protein that had been treated with papain prior to incubation with rabbit reticulocyte ribosomes (lanes 1 and 2) or protein corresponding to an active form of RIP1 (lanes 3 and 4). Aliquots of purified RNA from each reaction were prepared for electrophoresis (lanes 1 and 3) or treated with aniline before electrophoresis (lanes 2 and 4). The arrow indicates the small aniline cleavage product in samples treated with RIP and aniline.

which the first transcript was replaced by water (Fig. 10A). Next, a RIP-dependent inhibition of translation was observed, using a transcript from a recombinant active deletion mutant of RIP1 (Krawetz and Boston, 2000) as the first transcript (Fig. 10B, 'active RIP3:1'). The production of the active RIP1 blocked the production of the reporter protein, as expected for this previously characterized ribosome-inactivating protein. In the third experiment (Fig. 10C), the translation extract was first programmed with *Rip3:2* RNA, followed by the reporter zein transcript. The *Rip3:2* ORF (RIP2 ORF, filled arrowhead, Fig. 10C) transcript resulted in the accumulation of a product of the expected size (31 kDa, filled arrowhead). The subsequent appearance of the reporter zein protein indicated that the *Rip3:2* ORF-encoded protein did not inactivate the ribosomes. The zein was first detected at 25 min after addition of zein transcripts regardless of whether the *Rip3:2* gene product (proRIP2) was present or not. Thus, proRIP2, like proRIP1, is synthesized as an inactive zymogen or proenzyme. To test whether this *in vitro*-synthesized proRIP2 could still be proteolytically activated, as was the recombinant proRIP2, the cell-free translation reaction was fractionated to separate the soluble proRIP2 from the ribosomes. Treatment of the supernatant fraction with papain resulted in potent translational inhibitory activity, dependent on the presence of both proRIP2 and papain (JE Krawetz and RS Boston, unpublished results).

Discussion

Identification of the *Rip3:2* gene establishes that maize RIPs are encoded by multiple genes. The relationship between the loci for the two maize RIP genes was examined using recombinant inbred RFLP linkage mapping (Burr and Burr, 1991). Many genes in maize are present in two or

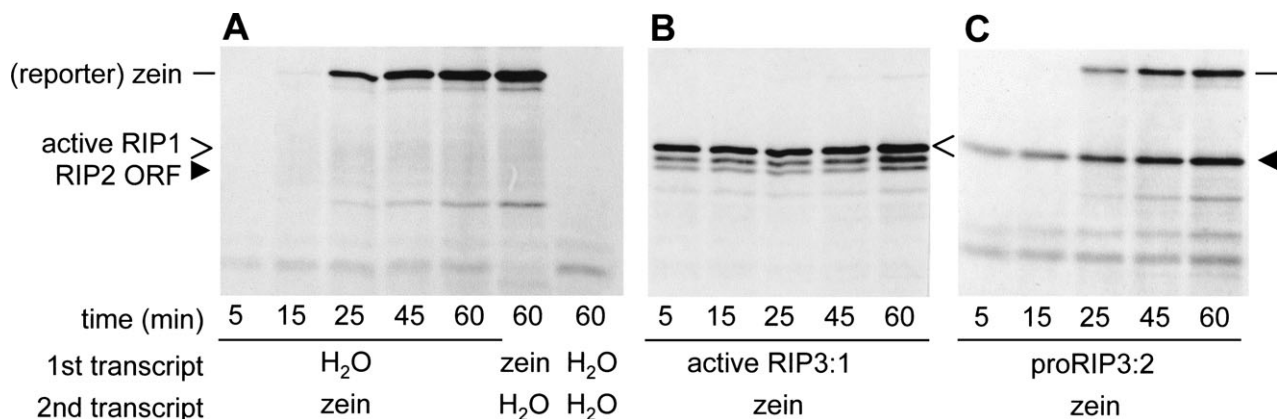


Fig. 10. Effect of proRIP2 on translation *in vitro*. Synthetic RNAs were translated in the presence of ^3H -Leu and ^{35}S -Met for 30 min prior to the addition of a 4-fold mass excess of a second, control (zein) transcript. Translation products were fractionated by SDS-PAGE and subjected to fluorography. The times listed below the panels indicate the length of incubation after the addition of the second transcript. Positions of the reporter zein (dashes), proRIP3:2 (open arrowheads), and deletion mutant active RIP3:1 (closed arrowheads) are indicated. The panels (A, B, and C) correspond to three different experiments; the combination of first and second transcripts is specified at the bottom.

more copies. Results from both cytogenetic and comparative mapping studies have led to the idea that maize is derived from a stabilized but rearranged ancient tetraploid (Helentjaris *et al.*, 1988; Whitkus *et al.*, 1992; Ahn and Tanksley, 1993). If the two RIP genes are homeologous loci, as is common in tetraploid species, one might expect to find them localized within known duplicated chromosome regions. Using both cross-hybridizing and gene-specific RIP probes, it was found that the *Rip3:2* and *Rip3:1* genes were unlinked. The *Rip3:2* probe hybridized to loci on chromosome 7L (Bass *et al.*, 1995) in bin 7.04 between the RFLP loci *BNL8.21A* and *BNL7.61*. The *Rip3:1* probe hybridized to loci on chromosome 8L (HW Bass and PH Sisco, unpublished results) in bin 8.05 between the RFLP loci *BNLACT1* and *BNL2.369*. The regions surrounding the two maize RIP map positions have not been identified as duplicated regions that reflect the ancient duplication of the genome (Helentjaris *et al.*, 1988; Whitkus *et al.*, 1992; Ahn and Tanksley, 1993; Gale and Devos, 1998; Wilson *et al.*, 1999; Gaut, 2001). The homology between *Rip3:1* and *Rip3:2* therefore appears to be more paralogous than orthologous, an observation that is consistent with their non-syntenic locations and their vastly different RNA expression patterns.

RNA encoding RIP2 was detected in more than 30 different RNA preparations including those from young and old leaves, roots, shoots, tassels, stems, seeds, and seedlings (Fig. 4; HW Bass, unpublished results). When tissues were collected from plants grown under normal field conditions, little evidence was found for significant accumulation of *Rip3:2* RNA in any particular tissue or developmental stage. This widespread pattern of RIP RNA expression in most plant parts appears to be unusual, as many RIPs exhibit a tissue-specific expression pattern, with pronounced accumulation in one particular part such as root, leaf, or seed.

Exposure of plants to drought stress resulted in a dramatic increase of *Rip3:2* RNA and proRIP2 protein levels. This induction was seen in both mature, field-grown material (Table 2) and immature seedlings (Fig. 7). Following removal of water stress, the *Rip3:2* transcripts in stressed plants returned to basal levels. The increase in *Rip3:2* RNA may not be a general stress response, however, as no change was observed in ears of plants grown under high-density stress (JE Habben and C Zinselmeier, unpublished results).

Accumulation of *Rip3:2* RNA and protein in response to drought or shading contrasts markedly with that of *Rip3:1* RNA, which accumulates specifically in the endosperm tissue during kernel development. Accumulation of *Rip3:1* RNA is primarily controlled by the transcriptional activator Opaque-2, but Opaque-2-independent expression has also been observed (Bass *et al.*, 1994; Muller *et al.*, 1997). Bass *et al.* (1994) found a significant effect of inbred background on *Rip3:1* RNA levels in the absence of the Opaque-2

protein, and Muller *et al.* (1997) found an increase in RIP1 (b-32) cross-reacting material in response to supplemental addition of amino acids, methyl jasmonate, ABA, cefotaxime, or nitrogen in an *opaque-2* culture system. Some of the cross-reacting material detected in the cultured endosperm may have been RIP2, but promoter-GUS fusions clearly showed an induction of the *Rip3:1*-promoter-GUS fusion by nitrogen (Muller *et al.*, 1997). Taken together, these results suggest that different but complex regulatory controls affect RIP gene expression in maize.

The differences in amino-acid sequences between proRIP1 and proRIP2 are located mostly in the regions that are proteolytically removed during proRIP activation. The internal amino-acid stretch between Block C and Block D (Fig. 1) is similarly located in the two RIPs and contains a tandem array of acidic, albeit different (aspartate rather than glutamate), residues. This internal sequence has been previously reported to be the primary determinant in inhibiting RIP activity in the proRIP1 (Hey *et al.*, 1995). This conclusion is based on a variety of proRIP deletion constructs tested by Hey *et al.* (1995). These authors analysed gene constructions lacking the NH₂-terminal, COOH-terminal, and internal regions in single, double, and triple mutant combinations for their RIP activity and relative activation upon protease treatment. In all cases, removal of the internal acidic region of proRIP1 resulted in activation of the enzyme. Thus, the presence of the internal acidic region (alone or in combination with the COOH-terminal region) is clearly responsible for the zymogen properties of the full-length polypeptide.

The internal acidic region could alter the arrangement of key residues in the active-site cleft. Formation of the active-site cleft is associated with the presence of a long central alpha helix (alpha 7 of trichosanthin, Helix E of ricin A-chain) that exhibits a peculiar 110° bend (Katzin *et al.*, 1991; Xiong *et al.*, 1994). A disruption of protein folding that would perturb the central helix containing the invariant residues E¹⁷⁷ and R¹⁸⁰ in (Block D of Fig. 1) might also result in an inactive RIP. Alternatively, the acidic region might act either by steric hindrance or competitive interaction with another molecule to block access by the ribosome to the active site. A third possibility is that the chemical attributes of the acidic residues themselves could affect the affinity of the RIP for its target substrate. Which, if any, of these possibilities serves to explain the lack of activity in proRIPs remains to be determined.

A high degree of antigenic similarity between RIPs from a single species is not universal. Seed and leaf forms of tritin, a wheat RIP, are antigenically unrelated, yet antiserum directed against the seed form of tritin cross-reacts with inhibitors from barley and rye seed (Massiah and Hartley, 1995). Several *Saponaria officinalis* seed RIPs cross-react with each other, but not with RIPs from other species (Lappi *et al.*, 1985). Two RIPs from carnation, dianthin 30 and dianthin 32, show weak cross-reactivity (Falasca *et al.*,

1982), and two RIPs from *Mirabilis expansa* roots had strong cross-reactivity (Vivanco *et al.*, 1999). Dianthin 30 is found in leaves and shoots, whereas dianthin 32 is found in stems, roots, and seeds as well (Reisbig and Bruland, 1983a). Pokeweed antiviral protein (PAP), a leaf RIP, is antigenically unrelated to a second leaf RIP, PAP-II, but anti-PAP antibodies do show weak cross-reaction with PAP-S from seeds and PAP-H from hairy root cultures of pokeweed (Irvin *et al.*, 1980; Barbieri *et al.*, 1982; Park *et al.*, 2002). Antiserum raised against maize proRIP1 cross-reacts well not only with maize proRIP2 (Fig. 7), but also with RIPs from closely related species such as tripsacum and sorghum (Hey *et al.*, 1995). RIPs from wheat, barley, and rye share epitopes among themselves but not with RIPs of maize (Reisbig and Bruland, 1983b). It remains to be determined whether the antigenic relationships reflect the variation in biological activity against potential target ribosomes.

Using primer extension analysis, two different sizes of extension products (~212 nt and ~216 nt) were identified depending on the source of the RNA (Fig. 5A). It was concluded from these results that it was possible to distinguish between the two RIP genes. Specifically, the 212 nt band was derived from *Rip3:1* and the 216 nt band from *Rip3:2*, assignments that are supported by the detection of the 216 nt product in a variety of plant RNAs, but of the 212 nt product only in kernel RNA. Furthermore, the detection of a doublet (both the 216 nt and 212 nt bands) in RNA from an endosperm suspension culture line allowed the possibility to be ruled out that the different apparent sizes were due to electrophoretic artefacts (HW Bass, GR O'Brien, and RS Boston, unpublished results). The predicted transcriptional start site of *Rip3:2* is also in agreement with the proRIP2 protein being smaller than proRIP1 (Fig. 7).

Comparison of the DNA sequences near the predicted transcriptional start sites of the *Rip3:1* and *Rip3:2* genes shows no significant stretches of similarity other than similarly placed TATA-like boxes, one at 34 nt upstream of the *Rip3:2* mRNA and 38 nt upstream of the *Rip3:1* mRNA (Hartings *et al.*, 1990). Furthermore, no binding sites for the Opaque-2 transcription factor (Lohmer *et al.*, 1991; Schmidt *et al.*, 1992) were found in a scan of approximately 300 nt 5' of the *Rip3:2* translation start site (HW Bass, GR O'Brien, and RS Boston, unpublished results). On the basis of these data and the marked differences in their expression patterns within the plant, the two maize RIP genes are most likely controlled by different transcriptional regulatory elements.

An important question remains to be answered: Is there any advantage to the plant in producing an inactive proRIP? Maize ribosomes themselves are resistant to the active form of RIP1 (Bass *et al.*, 1992; Hey *et al.*, 1995; Krawetz and Boston, 2000). ProRIP1 accounts for 1–3% of the soluble protein in mature maize seed (Soave *et al.*, 1981). During seed germination, no additional RIP cross-reacting material

is synthesized, but RIP activity increases dramatically with the onset of protease accumulation at approximately 3 d after germination (Bass *et al.*, 1992). The data presented here clearly indicate that RIP2 is synthesized as a proenzyme, but it is not known whether activation *in vivo* is caused by exposure to maize proteases or by exposure to proteases introduced by invading pests or pathogens or both. Polypeptides of similar sizes were produced by papain treatment of rRIP1 and rRIP2 (A Mehta and RS Boston, unpublished results). Nevertheless, RIP2 expression is not obviously linked to storage organs whose contents need to be protected or that produce a burst of proteolytic enzymes during the course of normal development.

A role for RIPs in plant defence has been investigated in a number of studies (reviewed in Nielsen and Boston, 2001). For example, in bioassays, purified maize RIP1 deterred insect feeding (Dowd *et al.*, 1998) and inhibited fungal growth (Nielsen *et al.*, 2001). Transgenic tobacco expressing the maize proRIP1, a modified active RIP1, or a barley RIP had more resistance to fungal invasion (Logeman *et al.*, 1992; Jach *et al.*, 1995; Maddaloni *et al.*, 1997; Kim *et al.*, 2003); those expressing a RIP from pokeweed or *Sambucus nigra* showed improved resistance to viral infection (Lodge *et al.*, 1993; Chen *et al.*, 2002); and those expressing a RIP from *Tricosanthes kirilowii* showed both antiviral and antifungal activities (Krishnan *et al.*, 2002; Yuan *et al.*, 2002). Even so, these findings do not rule out a role for RIPs in normal plant growth and development. Neale *et al.* (1990) showed that chitinase, β -1,3-glucanase, osmotin, and extensin were expressed in developmentally specific patterns in healthy plants. The authors point out that, although many of these proteins are pathogenesis-related, they may also be involved in normal developmental processes. Studies with a jasmonic-acid-induced protein (JIP60) from barley indicate that proteolytic processing of the protein confers RIP activity (Chaudhry *et al.*, 1994). The onset of JIP60 RNA accumulation in leaves showed a positive correlation with the abundance of monoribosomes and a negative correlation with accumulation of polyribosomes in tissues subjected to jasmonic acid or water stress (Reinbothe *et al.*, 1994a). Certain plants may, therefore, synthesize RIPs whose enzymatic activity is differentially regulated by factors associated with target ribosomes (Reinbothe *et al.*, 1994b).

The discovery of a second RIP in maize allows comparative analyses for the investigation of the functions they have in the plant and the factors regulating their accumulation. Both of the maize RIPs require proteolytic activation even though they accumulate to very different levels in the plant. Natural activation of proRIP1 by proteases produced during germination points to a likely biological activity to protect storage reserves from invading pests and pathogens. The advantage to the plant of having a second RIP induced

by water stress may be in improved non-host resistance at a time when the plant is vulnerable to pathogen attack.

Acknowledgements

We thank J Gillikin for excellent technical assistance, J Wallace and B Larkins for the modified zein clone – pMZ44-SV40, P Sisco for aid in RFLP mapping of the RIP clones; and members of the Boston laboratory for helpful comments during the course of this work. This work was supported by USDA grants 92-37304-7939 and 95-37304-2250 and NSF grant MCB-9307979 and the North Carolina Agricultural Research Service to RSB; a Department of Education GAANN fellowship to JEK; and the Florida State University Research Foundation Program Enhancement Grant to HWB.

References

- Ahn S, Tanksley SD. 1993. Comparative linkage maps of the rice and maize genomes. *Proceedings of the National Academy of Sciences, USA* **90**, 7980–7984.
- Ausubel FM, Brent R, Kingston RE, Moore DD, Seidman JG, Smith JA, Struhl K. 1992. *Current protocols in molecular biology*. New York: Greene Publishing Associates, Wiley-Interscience.
- Barbieri L, Stirpe F. 1982. Ribosome-inactivating proteins from plants: properties and possible uses. *Cancer Survey* **1**, 489–520.
- Barbieri L, Aron GM, Irvin JD, Stirpe F. 1982. Purification and partial characterization of another form of the antiviral protein from the seeds of *Phytolacca americana* L. (pokeweed). *Biochemical Journal* **203**, 55–59.
- Bass HW, OBrian GR, Boston RS. 1995. Cloning and sequencing of a second ribosome-inactivating protein gene from maize (*Zea mays* L.). *Plant Physiology* **107**, 661–662.
- Bass HW, Goode JH, Greene TW, Boston RS. 1994. Control of ribosome-inactivating protein (RIP) RNA levels during maize seed development. *Plant Science* **101**, 17–30.
- Bass HW, Webster C, OBrian GR, Roberts JK, Boston RS. 1992. A maize ribosome-inactivating protein is controlled by the transcriptional activator *Opaque-2*. *The Plant Cell* **4**, 225–234.
- Becker W, Apel K. 1992. Isolation and characterization of a cDNA clone encoding a novel jasmonate-induced protein of barley (*Hordeum vulgare* L.). *Plant Molecular Biology* **19**, 1065–1067.
- Bonner TI, Brenner DJ, Neufeld BR, Britten RJ. 1973. Reduction in the rate of DNA reassociation by sequence divergence. *Journal of Molecular Biology* **81**, 123–135.
- Boston RS, Larkins BA. 1986. Specific transcription of a 15 kilodalton zein gene in HeLa cell extracts. *Plant Molecular Biology* **7**, 71–79.
- Burr B, Burr FA. 1991. Recombinant inbreds for molecular mapping in maize; theoretical and practical considerations. *Trends in Genetics* **7**, 55–60.
- Casey J, Davidson N. 1977. Rates of formation and thermal stabilities of RNA:DNA and DNA:DNA duplexes at high concentrations of formamide. *Nucleic Acids Research* **4**, 1539–1552.
- Chaudhry B, Mueller-Uri F, Cameron-Mills V, Gough S, Simpson D, Skriver K, Mundy J. 1994. The barley 60 kDa jasmonate-induced protein (JIP60) is a novel ribosome-inactivating protein. *The Plant Journal* **6**, 815–824.
- Chen Y, Peumans WJ, Van Damme EJ. 2002. The *Sambucus nigra* type-2 ribosome-inactivating protein SNA-I' exhibits *in planta* antiviral activity in transgenic tobacco. *FEBS Letters* **516**, 27–30.
- Chevalier C, Bourgeois E, Pradet A, Raymond P. 1995. Molecular cloning and characterization of six cDNAs expressed during glucose starvation in excised maize (*Zea mays* L.) root tips. *Plant Molecular Biology* **28**, 473–485.
- Di Fonzo N, Manzocchi L, Salamini f, Soave C. 1986. Purification and properties of an endospermic protein of maize associated with the *opaque-2* and *opaque-6* genes. *Planta* **167**, 587–594.
- Di Fonzo N, Hartings H, Brembilla M, Motto M, Soave C, Navarro E, Palau J, Rhode W, Salamini F. 1988. The b-32 protein from maize endosperm, an albumin regulated by the O2 locus: nucleic acid (cDNA) and amino acid sequences. *Molecular and General Genetics* **212**, 481–487.
- Di Massimo AM, Di Loreto M, Pacilli A, Raucci G, D'Alatri L, Mele A, Bolognesi A, Polito L, Stirpe F, De Santis R. 1997. Immunoconjugates made of an anti-EGF receptor monoclonal antibody and type 1 ribosome-inactivating proteins from *Saponaria ocyroides* or *Vaccaria pyramidata*. *British Journal of Cancer* **75**, 822–828.
- Dowd PF, Mehta AD, Boston RS. 1998. Relative toxicity of the maize endosperm ribosome-inactivating protein to insects. *Journal of Agricultural and Food Chemistry* **46**, 3775–3779.
- Endo Y, Tsurugi K. 1987. RNA N-glycosidase activity of ricin A-chain. Mechanism of action of the toxic lectin ricin on eukaryotic ribosomes. *Journal of Biological Chemistry* **262**, 8128–8130.
- Endo Y, Mitsui K, Motizuki M, Tsurugi K. 1987. The mechanism of action of ricin and related toxic lectins on eukaryotic ribosomes. The site and the characteristics of the modification in 28S ribosomal RNA caused by the toxins. *Journal of Biological Chemistry* **262**, 5908–5912.
- Evensen G, Mathiesen A, Sundan A. 1991. Direct molecular cloning and expression of two distinct abrin A-chains. *Journal of Biological Chemistry* **266**, 6848–6852.
- Falasca A, Gasperi-Campani A, Abbondanza A, Barbieri L, Stirpe F. 1982. Properties of the ribosome-inactivating proteins gelonin, *Momordica charantia* inhibitor, and dianthins. *Biochemistry Journal* **207**, 505–509.
- Fordham-Skelton AP, Taylor PN, Hartley MR, Croy RR. 1991. Characterisation of saporin genes: *in vitro* expression and ribosome inactivation. *Molecular and General Genetics* **229**, 460–466.
- Frankel A, Schlossman D, Welsh P, Hertler A, Withers D, Johnston S. 1989. Selection and characterization of ricin toxin A-chain mutations in *Saccharomyces cerevisiae*. *Molecular and Cellular Biology* **9**, 415–420.
- French RR, Penney CA, Browning AC, Stirpe F, George AJ, Glennie MJ. 1995. Delivery of the ribosome-inactivating protein, gelonin, to lymphoma cells via CD22 and CD38 using bispecific antibodies. *British Journal of Cancer* **71**, 986–994.
- Funatsu G, Islam MR, Minami Y, Sung-Sil K, Kimura M. 1991. Conserved amino acid residues in ribosome-inactivating proteins from plants. *Biochimie* **73**, 1157–1161.
- Gale MD, Devos KM. 1998. Comparative genetics in the grasses. *Proceedings of the National Academy of Sciences, USA* **95**, 1971–1974.
- Gasperi-Campani A, Barbieri L, Battelli MG, Stirpe F. 1985. On the distribution of ribosome-inactivating proteins amongst plants. *Journal of Natural Products (Lloydia)* **48**, 446–454.
- Gaut BS. 2001. Patterns of chromosomal duplication in maize and their implications for comparative maps of the grasses. *Genome Research* **11**, 55–66.
- Habuka N, Kataoka J, Miyano M, Tsuge H, Ago H, Noma M. 1993. Nucleotide sequence of a genomic gene encoding tritin, a ribosome-inactivating protein from *Triticum aestivum*. *Plant Molecular Biology* **22**, 171–176.
- Hao Q, Van Damme EJ, Hause B, Barre A, Chen Y, Rouge P, Peumans WJ. 2001. Iris bulbs express type 1 and type 2 ribosome-inactivating proteins with unusual properties. *Plant Physiology* **125**, 866–876.

- Hartings H, Lazzaroni N, Marsan PA, Aragay A, Thompson R, Salamini F, Di Fonzo N, Palau J, Motto M.** 1990. The b-32 protein from maize endosperm: characterization of genomic sequences encoding two alternative central domains. *Plant Molecular Biology* **14**, 1031–1040.
- Hartley MR, Lord JM.** 1993. Structure, function and applications of ricin and related cytotoxic proteins. In: Grierson D, ed. *Biosynthesis and manipulation of plant products*. Glasgow: Chapman and Hall, 210–239.
- Hartley MR, Chaddock J, Bonness MS.** 1996. The structure and function of ribosome-inactivating proteins. *Trends in Plant Science* **1**, 254–260.
- Helentjaris T, Weber D, Wright S.** 1988. Identification of the genomic locations of duplicate nucleotide sequences in maize by analysis of restriction fragment length polymorphisms. *Genetics* **118**, 353–364.
- Henikoff S.** 1991. Playing with blocks: some pitfalls of forcing multiple alignments. *New Biology* **3**, 1148–1154.
- Henikoff S, Henikoff JG.** 1994. Protein family classification based on searching a database of blocks. *Genomics* **19**, 97–107.
- Hey TD, Hartley M, Walsh TA.** 1995. Maize ribosome-inactivating protein (b-32). Homologs in related species, effects on maize ribosomes, and modulation of activity by pro-peptide deletions. *Plant Physiology* **107**, 1323–1332.
- Hong Y, Saunders K, Hartley MR, Stanley J.** 1996. Resistance to geminivirus infection by virus-induced expression of dianthin in transgenic plants. *Virology* **220**, 119–127.
- Irvin JD, Kelly T, Robertus JD.** 1980. Purification and properties of a second antiviral protein from *Phytolacca americana* which inactivates eukaryotic ribosomes. *Archives of Biochemistry and Biophysics* **200**, 418–425.
- Jach G, Gornhardt B, Mundy J, Logemann J, Pinsdorf E, Leah R, Schell J, Maas C.** 1995. Enhanced quantitative resistance against fungal disease by combinatorial expression of different barley antifungal proteins in transgenic tobacco. *The Plant Journal* **8**, 97–109.
- Katzin BJ, Collins EJ, Robertus JD.** 1991. Structure of ricin A-chain at 2.5 Å. *Proteins* **10**, 251–259.
- Kim JK, Jang IC, Wu R, Zuo WN, Boston RS, Lee YH, Ahn IP, Nahm BH.** 2003. Co-expression of a modified maize ribosome-inactivating protein and a rice basic chitinase gene in transgenic rice plants confers enhanced resistance to sheath blight. *Transgenic Research* **12**, 475–484.
- Krawetz JE, Boston RS.** 2000. Substrate specificity of a maize ribosome-inactivating protein differs across diverse taxa. *European Journal of Biochemistry* **267**, 1966–1974.
- Krishnan R, McDonald KA, Dandekar AM, Jackman AP, Falk B.** 2002. Expression of recombinant tricosanthin, a ribosome-inactivating protein, in transgenic tobacco. *Journal of Biotechnology* **97**, 69–88.
- Lamb FI, Roberts LM, Lord JM.** 1985. Nucleotide sequence of cloned cDNA coding for preproricin. *European Journal of Biochemistry* **148**, 265–270.
- Langridge P, Pintor-Toro JA, Feix G.** 1982. Transcriptional effects of the opaque-2 mutation of *Zea mays* L. *Planta* **156**, 166–170.
- Lappi DA, Esch FS, Barbieri L, Stirpe F, Soria M.** 1985. Characterization of a *Saponaria officinalis* seed ribosome-inactivating protein: immunoreactivity and sequence homologies. *Biochemistry and Biophysics Research Communications* **129**, 934–942.
- Leah R, Tommerup H, Svendsen I, Mundy J.** 1991. Biochemical and molecular characterization of three barley seed proteins with antifungal properties. *Journal of Biological Chemistry* **266**, 1564–1573.
- Legname G, Bellosta P, Gromo G, Modena D, Keen JN, Roberts LM, Lord JM.** 1991. Nucleotide sequence of cDNA coding for dianthin 30, a ribosome inactivating protein from *Dianthus caryophyllus*. *Biochimica et Biophysica Acta* **1090**, 119–122.
- Lin Q, Chen ZC, Antoniw JF, White RF.** 1991. Isolation and characterization of a cDNA clone encoding the anti-viral protein from *Phytolacca americana*. *Plant Molecular Biology* **17**, 609–614.
- Lodge JK, Kaniewski WK, Tumer NE.** 1993. Broad-spectrum virus resistance in transgenic plants expressing pokeweed antiviral protein. *Proceedings of the National Academy of Sciences, USA* **90**, 7089–7093.
- Logeman J, Jach G, Tommerup H, Mundy J, Schell J.** 1992. Expression of a barley ribosome-inactivating protein leads to increased fungal protection in transgenic tobacco plants. *Bio/Technology* **10**, 305–308.
- Lohmer S, Maddaloni M, Motto M, Di Fonzo N, Hartings H, Salamini F, Thompson RD.** 1991. The maize regulatory locus Opaque-2 encodes a DNA-binding protein which activates the transcription of the b-32 gene. *The EMBO Journal* **10**, 617–624.
- Maddaloni M, Forlani F, Balmas V, Donini G, Stasse L, Corazza L, Motto M.** 1997. Tolerance to the fungal pathogen *Rhizoctonia solani* AG4 of transgenic tobacco expressing the maize ribosome-inactivating protein b-32. *Transgenic Research* **6**, 393–402.
- Maniatis T, Fritsch EF, Sambrook J.** 1982. *Molecular cloning: a laboratory manual*. New York: Cold Spring Harbor Laboratory Press.
- Massiah AJ, Hartley MR.** 1995. Wheat ribosome-inactivating proteins: seed and leaf forms with different specificities and cofactor requirements. *Planta* **197**, 633–640.
- May MJ, Hartley MR, Roberts LM, Krieg PA, Osborn RW, Lord JM.** 1989. Ribosome inactivation by ricin A chain: a sensitive method to assess the activity of wild-type and mutant polypeptides. *EMBO Journal* **8**, 301–308.
- Montfort W, Villafranca JE, Monzingo AF, Ernst SR, Katzin B, Rutenber E, Xuong NH, Hamlin R, Robertus JD.** 1987. The three-dimensional structure of ricin at 2.8 Å. *Journal of Biological Chemistry* **262**, 5398–5403.
- Muller M, Dues G, Balconi C, Salamini F, Thompson RD.** 1997. Nitrogen and hormonal responsiveness of the 22 kDa alpha-zein and b-32 genes in maize endosperm is displayed in the absence of the transcriptional regulator Opaque-2. *The Plant Journal* **12**, 281–291.
- Mundy J, Leah R, Boston RS, Endo Y, Stirpe F.** 1994. Genes encoding ribosome-inactivating proteins. *Plant Molecular Biology Reports (Commission on Plant Gene Nomenclature Supplement)* **12**, S60–S62.
- Neale AD, Wahleithner JA, Lund M, Bonnett HT, Kelly A, Meeks-Wagner DR, Peacock WJ, Dennis ES.** 1990. Chitinase, beta-1, 3-glucanase, osmotin, and extensin are expressed in tobacco explants during flower formation. *The Plant Cell* **2**, 673–684.
- Nielsen K, Boston RS.** 2001. Ribosome-inactivating proteins: a plant perspective. *Annual Review of Plant Physiology and Plant Molecular Biology* **52**, 785–816.
- Nielsen K, Payne GA, Boston RS.** 2001. Maize ribosome-inactivating protein inhibits normal development of *Aspergillus nidulans* and *Aspergillus flavus*. *Molecular Plant–Microbe Interactions* **14**, 164–172.
- Park SW, Lawrence CB, Linden JC, Vivanco JM.** 2002. Isolation and characterization of a novel ribosome-inactivating protein from root cultures of pokeweed and its mechanism of secretion from roots. *Plant Physiology* **130**, 164–178.
- Peattie DA.** 1979. Direct chemical method for sequencing RNA. *Proceedings of the National Academy of Sciences, USA* **76**, 1760–1764.
- Poyet J-L, Radom J, Hoeveler A.** 1994. Isolation and characterization of a cDNA clone encoding the pokeweed antiviral protein II from *Phytolacca americana* and its expression in *E. coli*. *FEBS Letters* **347**, 268–272.

- Ready MP, Kim Y, Robertus JD.** 1991. Site-directed mutagenesis of ricin A-chain and implications for the mechanism of action. *Proteins* **10**, 270–278.
- Reinbothe S, Mollenhauer B, Reinbothe C.** 1994b. JIPs and RIPs: the regulation of plant gene expression by jasmonates in response to environmental cues and pathogens. *The Plant Cell* **6**, 1197–1209.
- Reinbothe S, Reinbothe C, Lehmann J, Becker W, Apel K, Parthier B.** 1994a. JIP60, a methyl jasmonate-induced ribosome-inactivating protein involved in plant stress reactions. *Proceedings of the National Academy of Sciences, USA* **91**, 7012–7016.
- Reisbig RR, Bruland O.** 1983a. Dianthin 30 and 32 from *Dianthus caryophyllus*: two inhibitors of plant protein synthesis and their tissue distribution. *Archives of Biochemistry and Biophysics* **224**, 700–706.
- Reisbig RR, Bruland O.** 1983b. The protein synthesis inhibitors from wheat, barley, and rye have identical antigenic determinants. *Biochemistry and Biophysics Research Communications* **114**, 190–196.
- Schmidt RJ, Ketudat M, Aukerman MJ, Hoschek G.** 1992. Opaque-2 is a transcriptional activator that recognizes a specific target site in 22-kD zein genes. *The Plant Cell* **4**, 689–700.
- Saave C, Tardani L, Di Fonzo N, Salamini F.** 1981. Zein level in maize endosperm depends on a protein under control of the opaque-2 and opaque-6 loci. *Cell* **27**, 403–410.
- Southern EM.** 1975. Detection of specific sequences among DNA fragments separated by gel electrophoresis. *Journal of Molecular Biology* **98**, 503–517.
- Stirpe F, Barbieri L.** 1986. Ribosome-inactivating proteins up to date. *FEBS Letters* **195**, 1–8.
- Stirpe F, Barbieri L, Battelli MG, Soria M, Lappi DA.** 1992. Ribosome-inactivating proteins from plants: present status and future prospects. *Bio/Technology* **10**, 405–412.
- Strockbine NA, Jackson MP, Sung LM, Holmes RK, O'Brien AD.** 1988. Cloning and sequencing of the genes for Shiga toxin from *Shigella dysenteriae* type 1. *Journal of Bacteriology* **170**, 1116–1122.
- van Damme EJ, Hao Q, Chen Y, Barre A, Vandenbussche F, Desmyter S, Rouge P, Peumans WJ.** 2001. Ribosome-Inactivating Proteins: a family of plant proteins that do more than inactivate ribosomes. *Critical Reviews in Plant Sciences* **20**, 395–465.
- Veronese P, Ruiz MT, Coca MA, et al.** 2003. In defense against pathogens. Both plant sentinels and foot soldiers need to know the enemy. *Plant Physiology* **131**, 1580–1590.
- Vilardell J, Goday A, Freire MA, Torrent M, Martinez MC, Torne JM, Pages M.** 1990. Gene sequence, developmental expression, and protein phosphorylation of RAB-17 in maize. *Plant Molecular Biology* **14**, 423–432.
- Vivanco JM, Savary BJ, Flores HE.** 1999. Characterization of two novel type I ribosome-inactivating proteins from the storage roots of the Andean crop *Mirabilis expansa*. *Plant Physiology* **119**, 1447–1456.
- Wallace JC, Galili G, Kawata EE, Cuellar RE, Shotwell MA, Larkins BA.** 1988. Aggregation of lysine-containing zeins into protein bodies in *Xenopus* oocytes. *Science* **240**, 662–664.
- Walsh TA, Morgan AE, Hey TD.** 1991. Characterization and molecular cloning of a proenzyme form of a ribosome-inactivating protein from maize. Novel mechanism of proenzyme activation by proteolytic removal of a 2.8-kilodalton internal peptide segment. *Journal of Biological Chemistry* **266**, 23422–23427.
- Weston SA, Tucker AD, Thatcher DR, Derbyshire DJ, Pauptit RA.** 1994. X-ray structure of recombinant ricin A-chain at 1.8 Å resolution. *Journal of Molecular Biology* **244**, 410–422.
- Wetmur JG, Davidson N.** 1968. Kinetics of renaturation of DNA. *Journal of Molecular Biology* **31**, 349–370.
- Whitkus R, Doebley J, Lee M.** 1992. Comparative genome mapping of sorghum and maize. *Genetics* **132**, 1119–1130.
- Wilson WA, Harrington SE, Woodman WL, Lee M, Sorrells ME, McCouch SR.** 1999. Inferences on the genome structure of progenitor maize through comparative analysis of rice, maize and the domesticated panicoids. *Genetics* **153**, 453–473.
- Wool IG, Gluck A, Endo Y.** 1992. Ribotoxin recognition of ribosomal RNA and a proposal for the mechanism of translocation. *Trends in Biochemical Science* **17**, 266–269.
- Xiong J-P, Xia, Z-X, Wang Y.** 1994. Crystal structure of trichosanthin-NADPH complex at 1.7 Å resolution reveals active-site architecture. *Nature Structural and Molecular Biology* **1**, 695–700.
- Yuan H, Ming X, Wang L, Hu P, An C, Chen Z.** 2002. Expression of a gene encoding tricosanthin in transgenic rice plants enhances resistance to fungus blast disease. *Plant Cell Reports* **20**, 992–998.
- Zimmer EA, Newton KJ.** 1982. A simple method for the isolation of high molecular weight DNA from individual maize seedlings and tissues. In: Sherdian WF, ed. *Maize for biological research*. Grand Forks, ND: North Dakota Press.
- Zoubenko O, Hudak K, Tumer NE.** 2000. A non-toxic pokeweed antiviral protein mutant inhibits pathogen infection via a novel salicylic acid-independent pathway. *Plant Molecular Biology* **44**, 219–229.